Supporting Information

Manipulating the cross-layer channels in *g*-C_3N_4 nanosheet membranes for enhanced molecular transport

Xiaoli Wu[a,1], Xulin Cui[a,1], Qi Wang[a], Jingtao Wang[a,b,*], Wenjia Wu[a], Wenpeng Li[a], Zhongyi Jiang[c,d,*]

[a]School of Chemical Engineering, Zhengzhou University, Zhengzhou 450001, P. R. China.

[b]Henan Institutes of Advanced Technology, Zhengzhou University, 97 Wenhua Road, Zhengzhou 450003, P. R. China

[c]Key Laboratory for Green Chemical Technology of Ministry of Education, School of Chemical Engineering and Technology, Tianjin University, Tianjin 300072, China.

[d]Collaborative Innovation Center of Chemical Science and Engineering (Tianjin), Tianjin 300072, China.

*To whom correspondence should be addressed: E-mail: zhyjiang@tju.edu.cn (Z.Y. Jiang); jingtaowang@zzu.edu.cn (J.T. Wang).

[1]These authors contributed equally to this work.

1. Experimental Methods

Note S1 Theoretical simulations

The analysis of the different geometries was carried out using the density functional theory (DFT) calculations by Cambridge Series of Total Energy Package (CASTEP) module of Accelrys Materials Studio with norm-conserving pseudo-potentials. The plane-wave cutoff energy was set to 500 eV and the Monkhorst–Pack *k*-meshes 12 × 12 × 1 were adopted for single-layer C_3N_4. The energy was calculated by applying the generalized gradient approximation (GGA) and Perdew–Burke–Ernzerhof (PBE). To study stabilities of the structures, the binding energies of OH groups on the edge and basal C and N atoms were calculated accordingly, and the expression of binding energy was calculated as

$$E_{binding} = \frac{E_{tot} - nE_{atom}}{n},$$

where E_{tot} is total energy of C_3N_4, and E_{atom} is the energy of single atoms, which is obtained by calculating the energies of isolated atoms in a cubic structure with lattice constant set as 10 Å to avoid interactions between neighboring atoms; n is the total number of atoms per unit cell.

Note S2 Calculation of the transmembrane resistance

The transmembrane resistance for a solvent transport through a lamellar membrane is calculated according to the equation: $R_s=1/P_s$, where R_s and P_s represent the resistance and permeance of a solvent, respectively.

Note S3 Calculation of the cross-layer channel size

Here, to calculate the size of cross-layer channels expediently, we assume that the nanosheets are square with different side length, and these squares are at the same plane for one of the layer in lamellar structure. Since the membranes have similar thickness and interlayer channel size, the layer numbers in these membranes are close. Therefore, cross-layer channel length is represented by the relative total perimeter of these squares that compose one of the layer plane in lamellar membrane.

Accordingly, the cross-layer channel size $L = 4S/a$, where L is the total perimeter, S is the area of one layer within membrane, and a is the side length of a square nanosheet.

2. Supplementary Figures

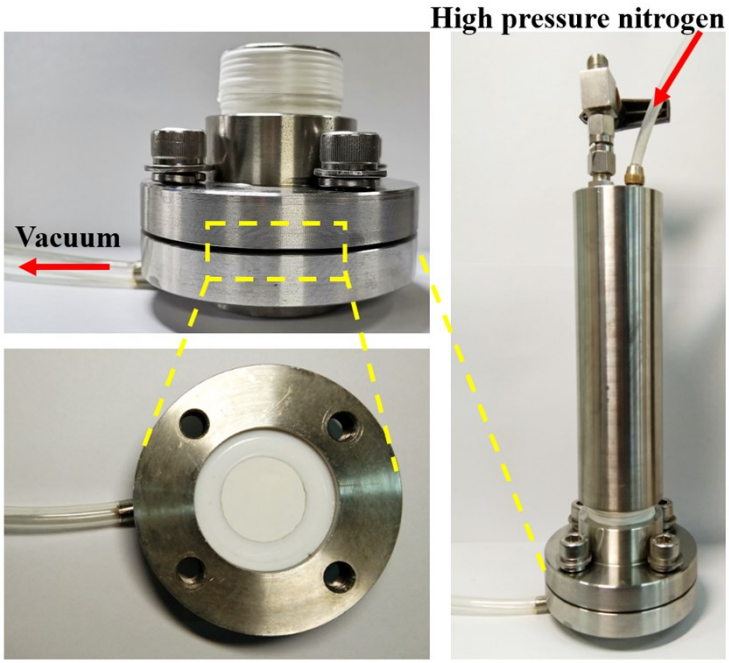

Fig. S1. The home-made experimental apparatus for the preparation and performance measurement of the membranes.

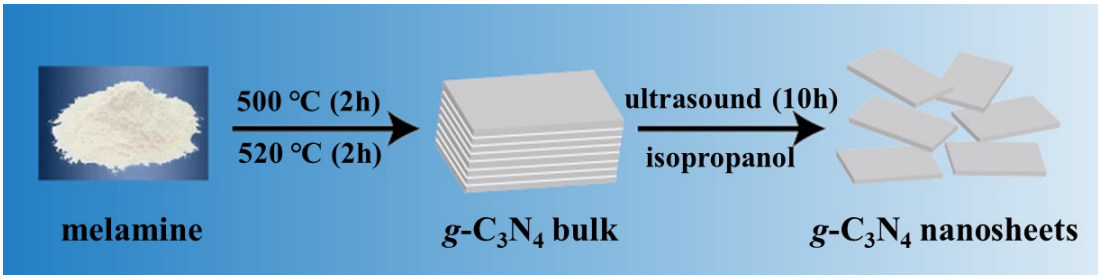

Fig. S2. Schematic illustration of the synthesis of *g*-C_3N_4 nanosheets.

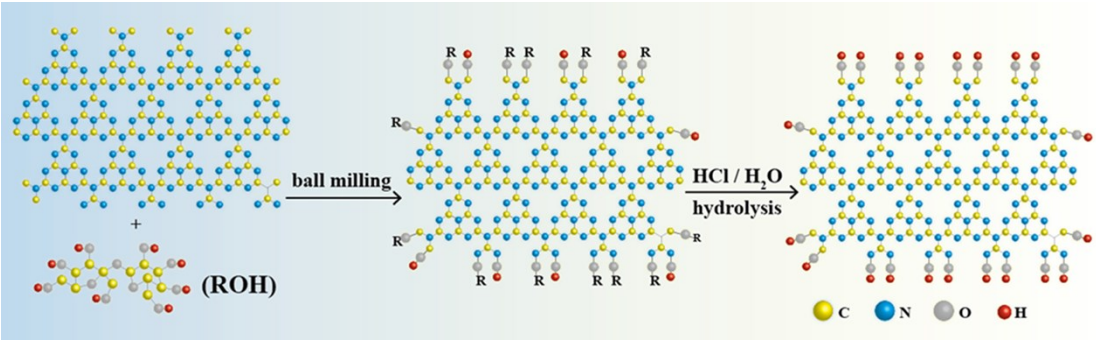

Fig. S3. Schematic illustration of the preparation of *g*-C_3N_4-OH nanosheets.

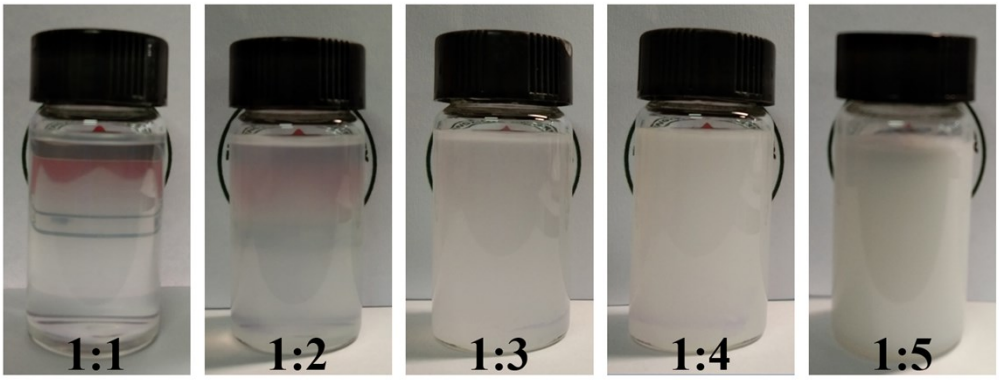

Fig. S4. Digital images of nanosheets dispersed in water with different mass ratios of *g*-C_3N_4/sucrose.

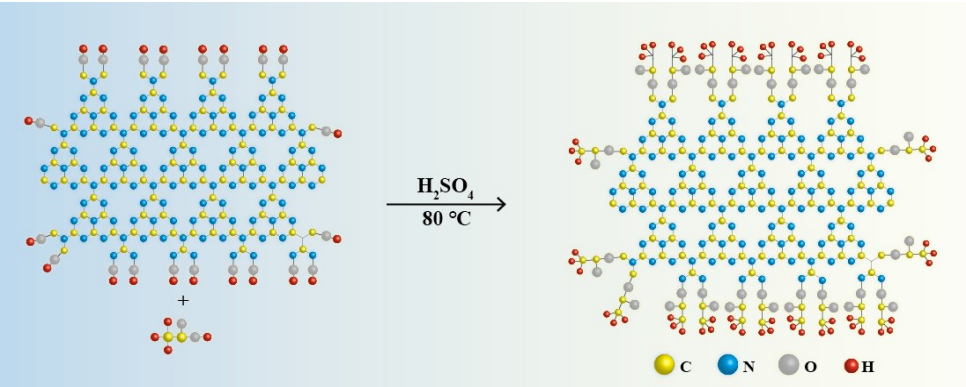

Fig. S5. Schematic illustration of the preparation of *g*-C_3N_4-$OOCCH_3$ nanosheets.

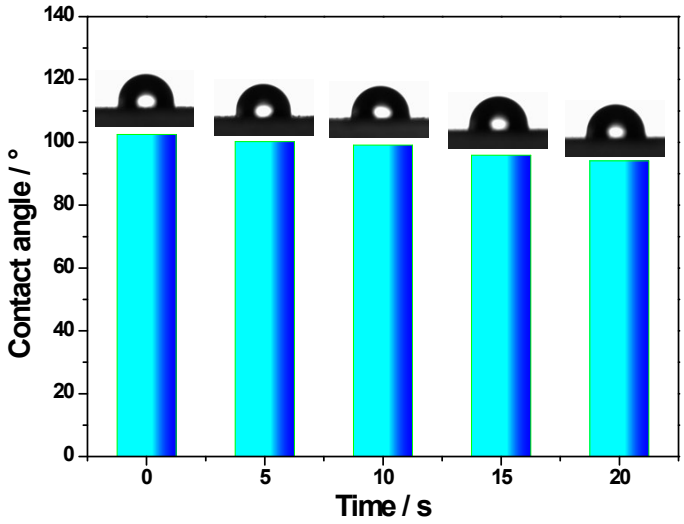

Fig. S6. Water contact angles of *g*-C_3N_4-$OOCCH_3$ tablets pressed by bead machine.

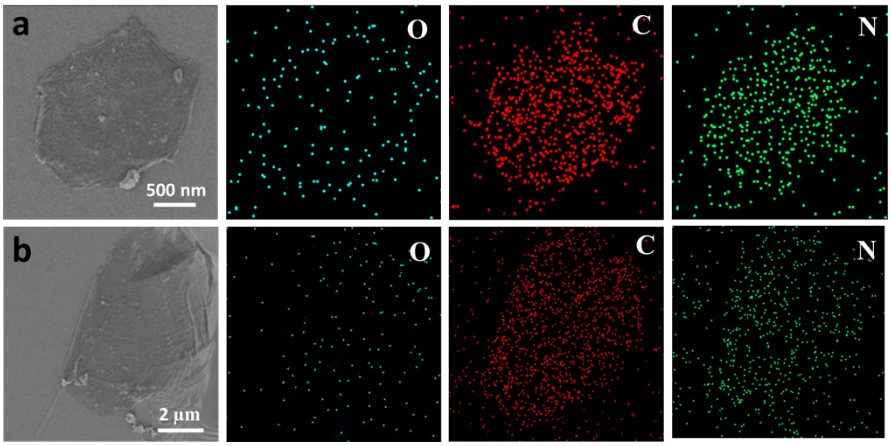

Fig. S7. SEM images and corresponding elemental mappings of O, N, and C for (a) *g*-C_3N_4-OH and (b) *g*-C_3N_4 nanosheets.

As for *g*-C_3N_4 nanosheets, the EDS mappings exhibit the typical C and N elements. And meanwhile, a certain amount of O elements also appear and evenly dispersed on the in-plane of nanosheets, which are introduced by the solvent of isopropanol during synthesis procedure. As contrast, more O elements are observed for *g*-C_3N_4-OH nanosheets and mainly dispersed on the edges, confirming that the -OH groups are grafted on the edges of nanosheets.

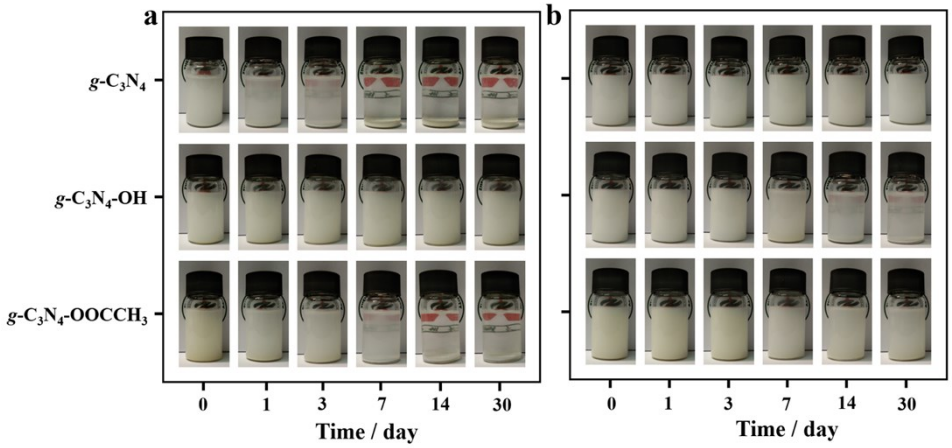

Fig. S8. Digital images of nanosheets dispersed in (a) water and (b) isopropanol.

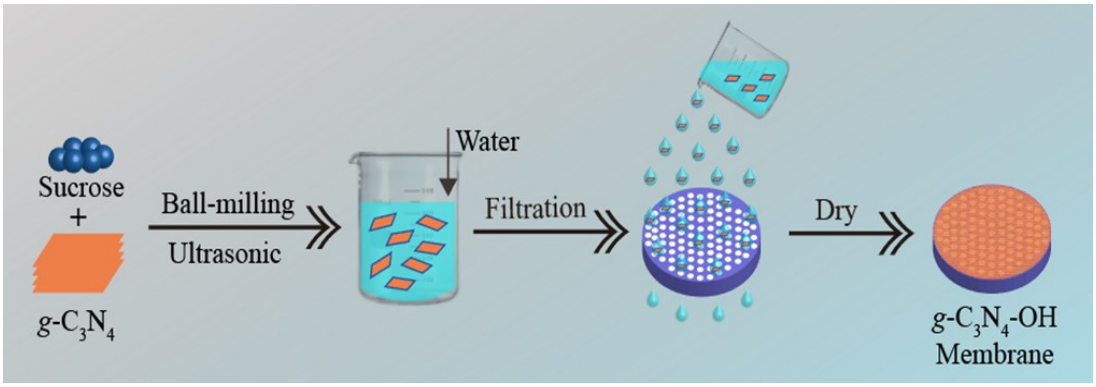

Fig. S9. Schematic illustration of the fabrication of *g*-C_3N_4-OH membrane.

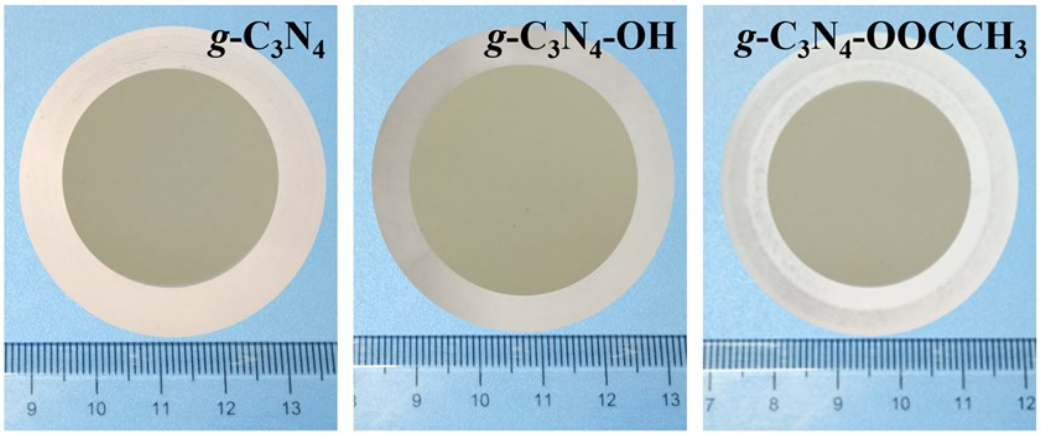

Fig. S10. Digital images of *g*-C_3N_4, *g*-C_3N_4-OH, and *g*-C_3N_4-$OOCCH_3$ membranes.

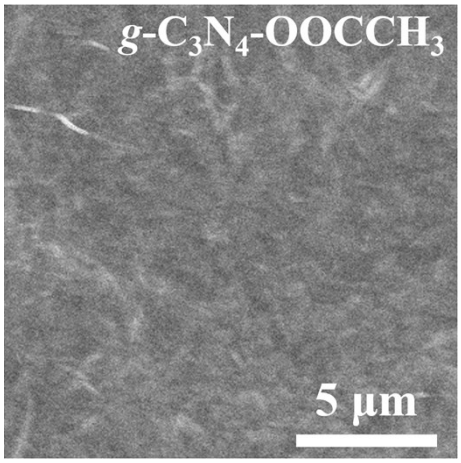

Fig. S11. Surface SEM image of *g*-C_3N_4-$OOCCH_3$ membrane.

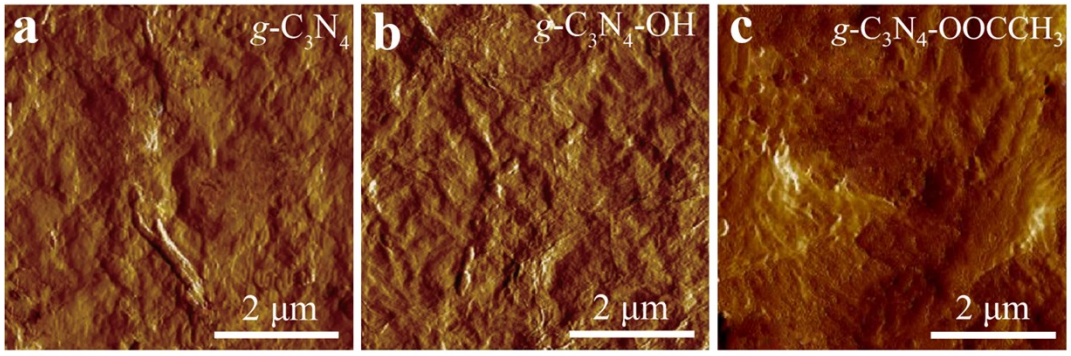

Fig. S12. AFM images of (a) *g*-C_3N_4, (b) *g*-C_3N_4-OH, and (c) *g*-C_3N_4-$OOCCH_3$ membranes.

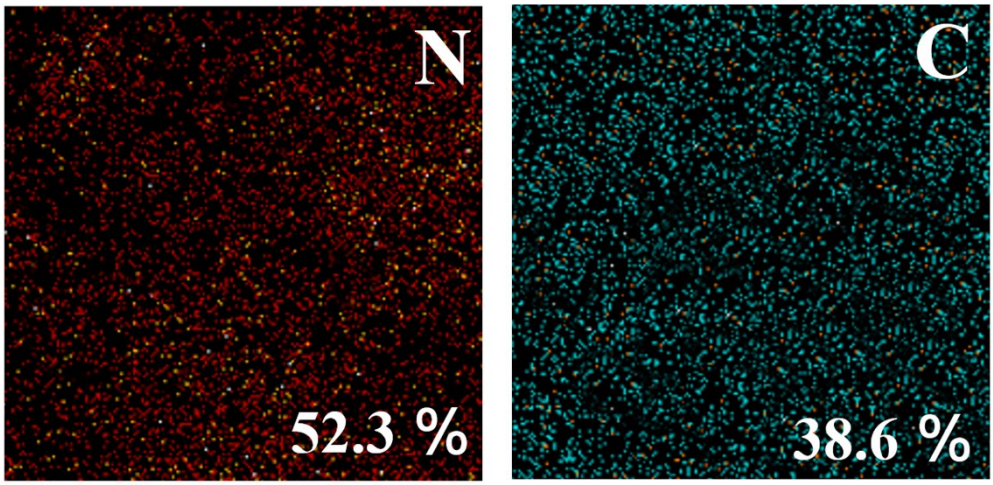

Fig. S13. Elemental mappings of N and C for *g*-C_3N_4-OH membrane.

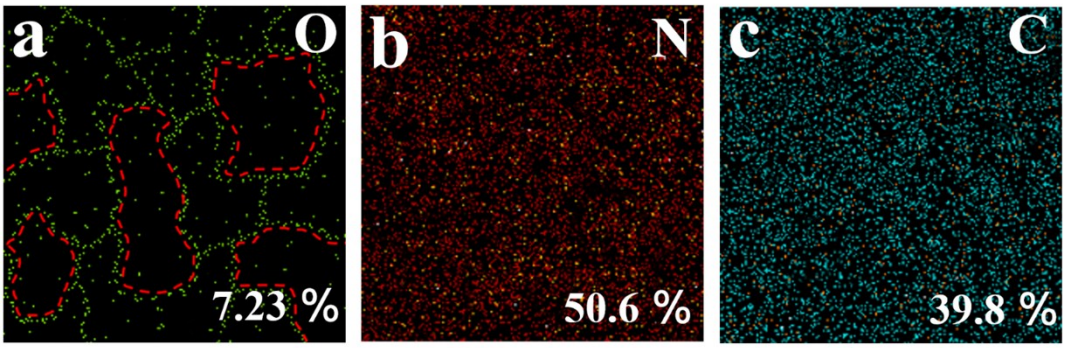

Fig. S14. Elemental mappings of O, N and C for *g*-C_3N_4-$OOCCH_3$ membrane.

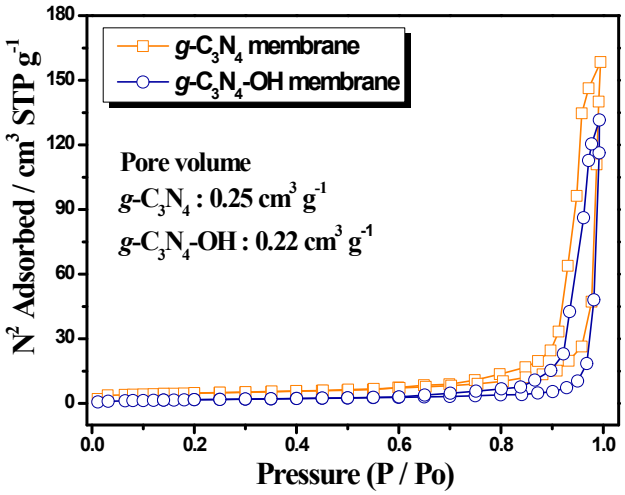

Fig. S15. N_2 sorption isotherms measured for *g*-C_3N_4 and *g*-C_3N_4-OH membranes.

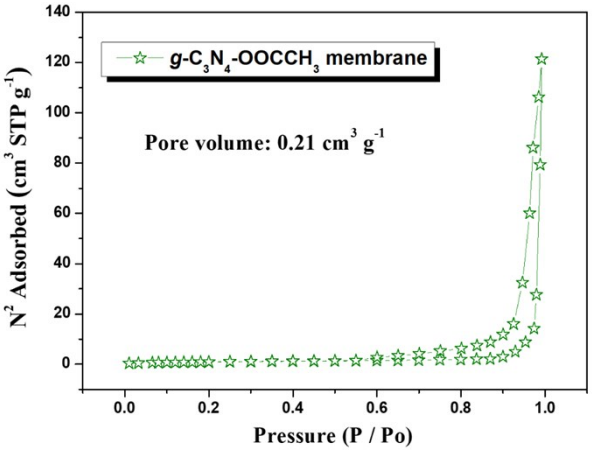

Fig. S16. N_2 sorption isotherms measured for *g*-C_3N_4-$OOCCH_3$ membrane.

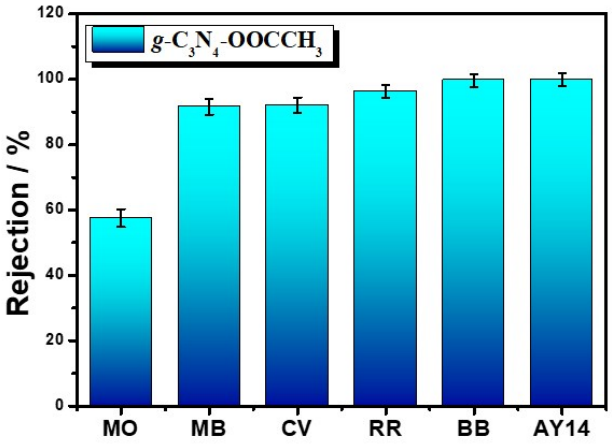

Fig. S17. Dye rejection for *g*-C_3N_4-$OOCCH_3$ membrane.

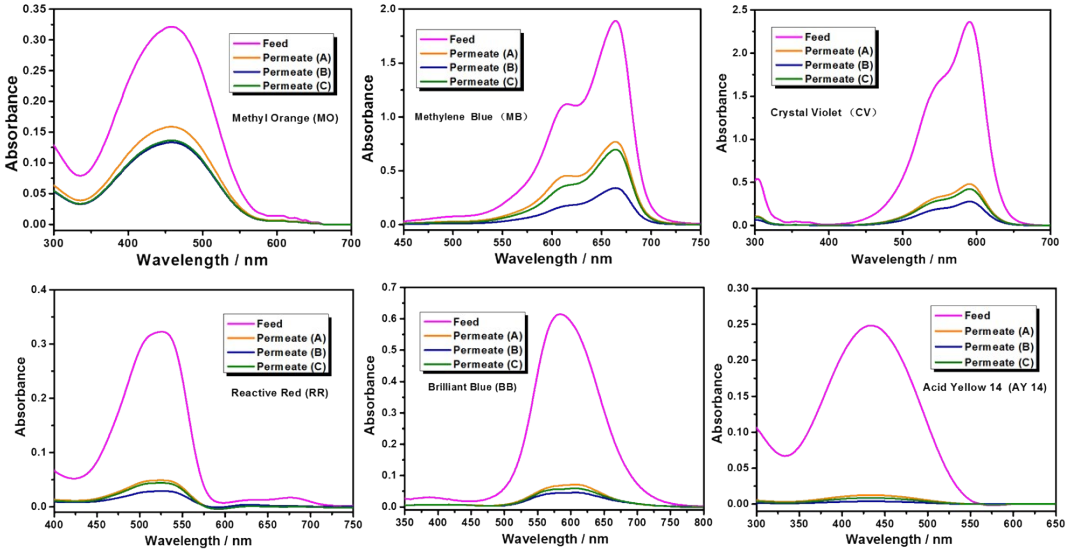

Fig. S18. UV-vis absorption spectra of dyes with different sizes in methanol before and after filtration through (A) *g*-C_3N_4, (B) *g*-C_3N_4-OH and (C) *g*-C_3N_4-$OOCCH_3$ membranes.

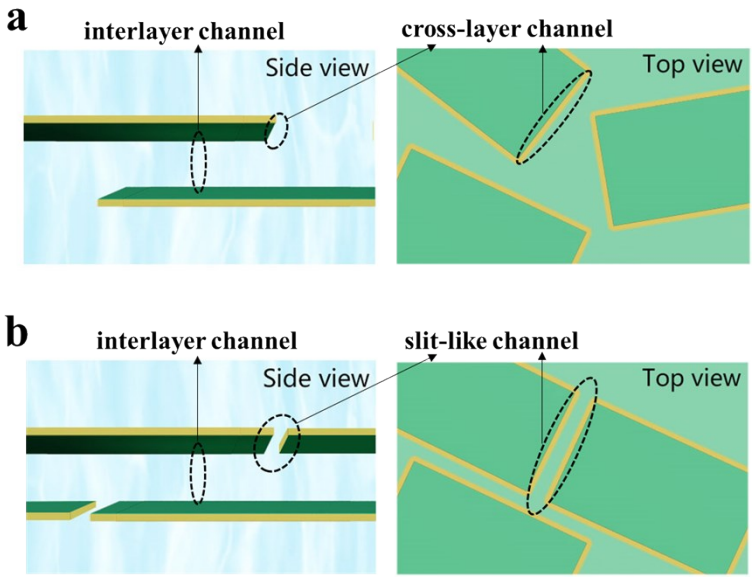

Fig. S19. Schematic illustration of interlayer channels and cross-layer channels in *g*-C_3N_4-OH membrane. Most nanosheets are cross-stacked to form (a) cross-layer channels, while few stacked to form (b) slit-like channels.

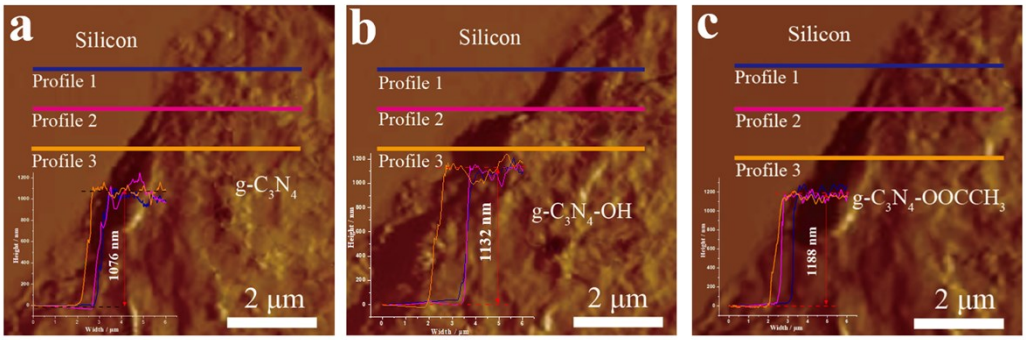

Fig. S20. AFM height images of (a) *g*-C_3N_4, (b) *g*-C_3N_4-OH, and (c) *g*-C_3N_4-$OOCCH_3$ membranes.

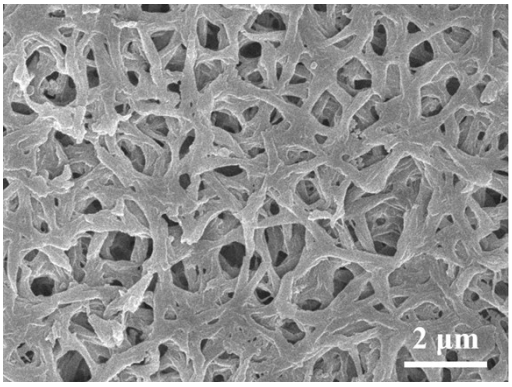

Fig. S21. SEM image of Nylon support.

Nylon support is widely used for the preparation of lamellar membranes due to its smooth surface and good chemical stability. [1-3]

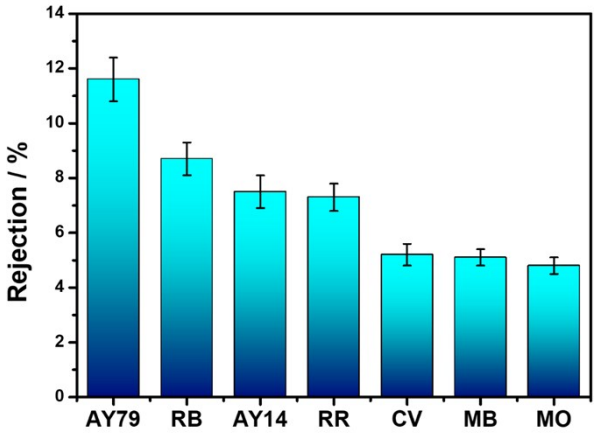

Fig. S22. Rejection of different dye molecules of Nylon support.

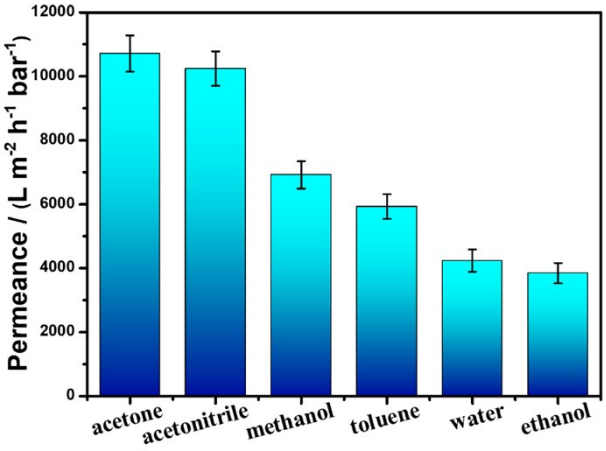

Fig. S23. Solvent permeance of nylon support.

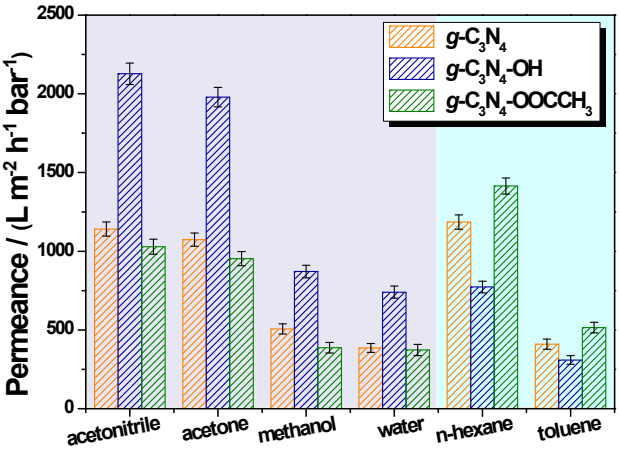

Fig. S24. Solvent permeance for membranes.

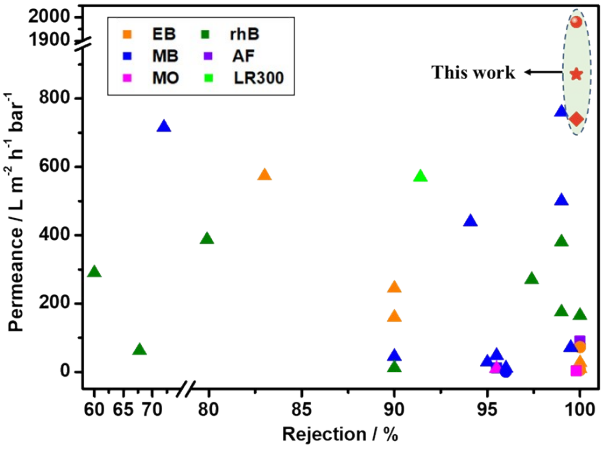

Fig. S25. Performance comparison for *g*-C_3N_4-OH membranes with various previously reported membranes (detailed information about those membranes are listed in Table S2).

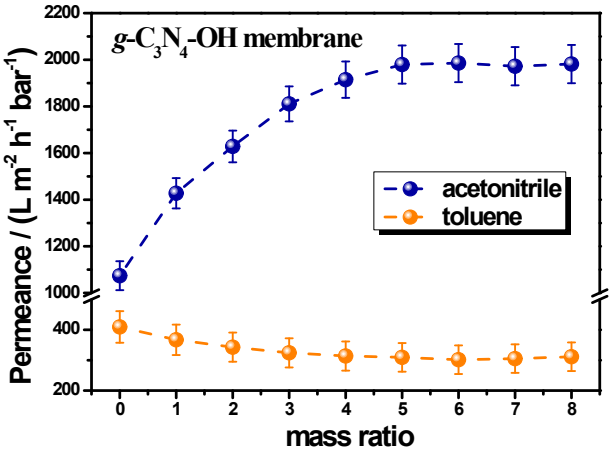

Fig. S26. Solvent permeance as a function of grafted -OH groups for *g*-C_3N_4-OH membrane.

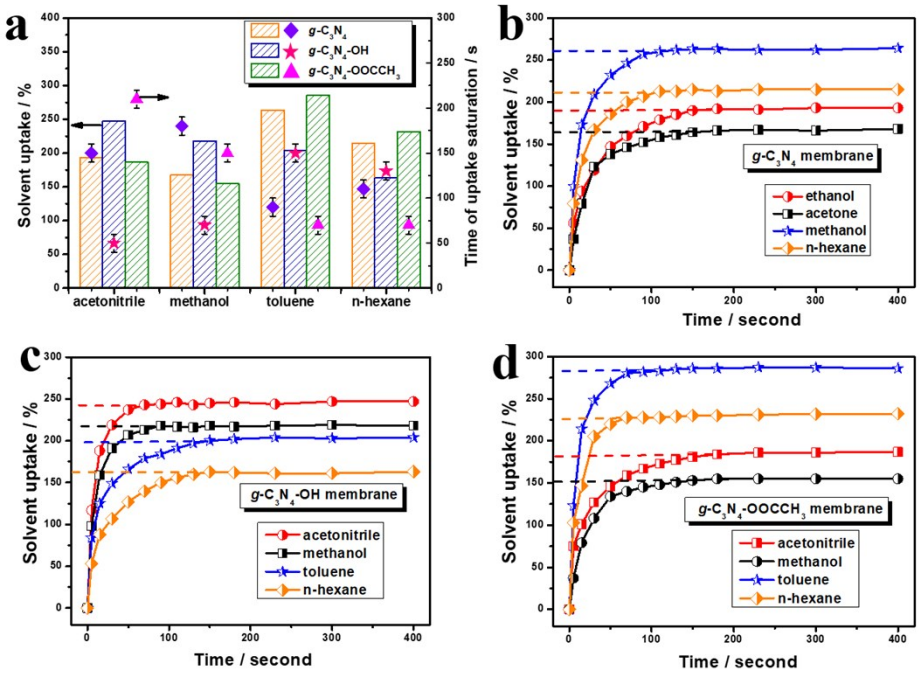

Fig. S27. (a) Saturated adsorption time and solvent uptake of membranes. Adsorption balance of (b) *g*-C_3N_4, (c) *g*-C_3N_4-OH and (d) *g*-C_3N_4-$OOCCH_3$ membranes in acetonitrile, methanol, toluene and n-hexane solvents.

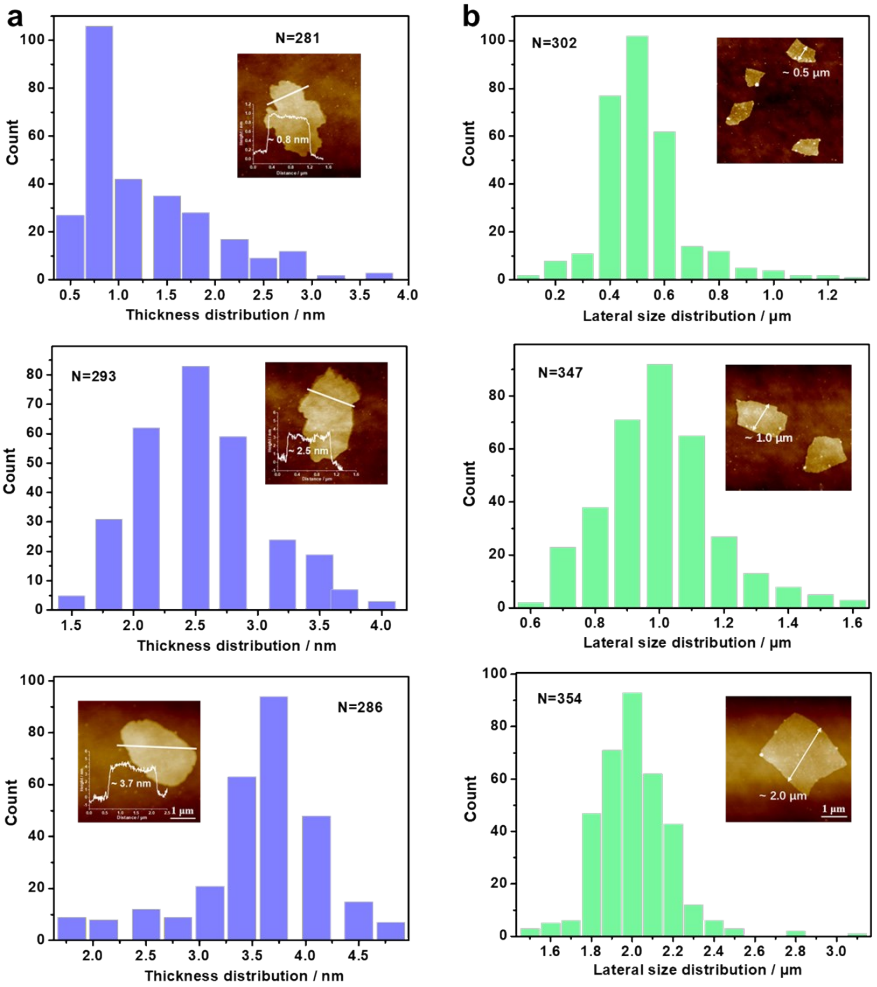

Fig. S28. (a) Thickness and (b) lateral size distribution of *g*-C_3N_4-OH nanosheets, as investigated using AFM over 280 nanosheets. Nanosheets deposited on silicon substrate are marked and analyzed.

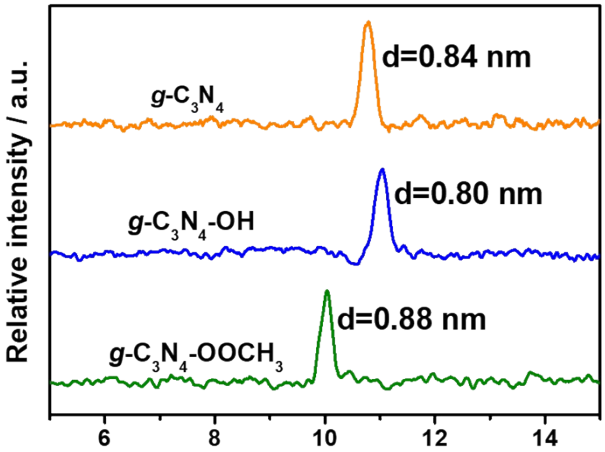

Fig. S29. XRD patterns of *g*-C_3N_4, *g*-C_3N_4-OH, and *g*-C_3N_4-$OOCH_3$ membranes dried in the air.

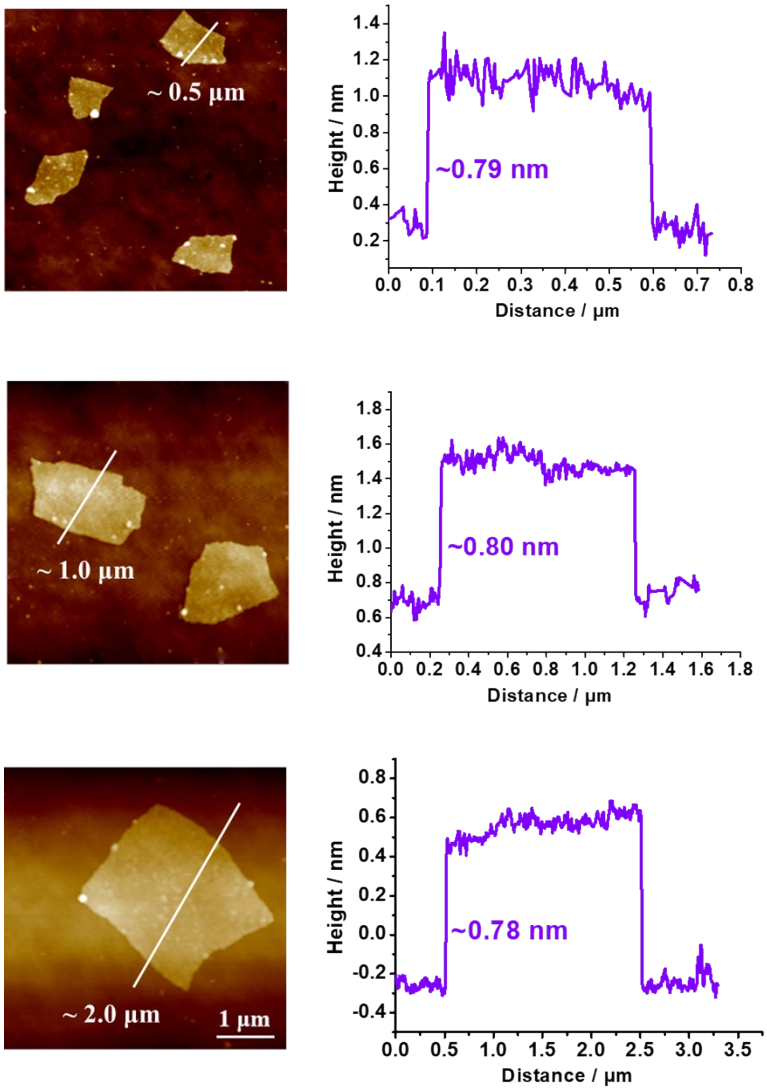

Fig. S30. AFM images of *g*-C_3N_4-OH nanosheets with close thickness and different lateral size, and the corresponding height profiles.

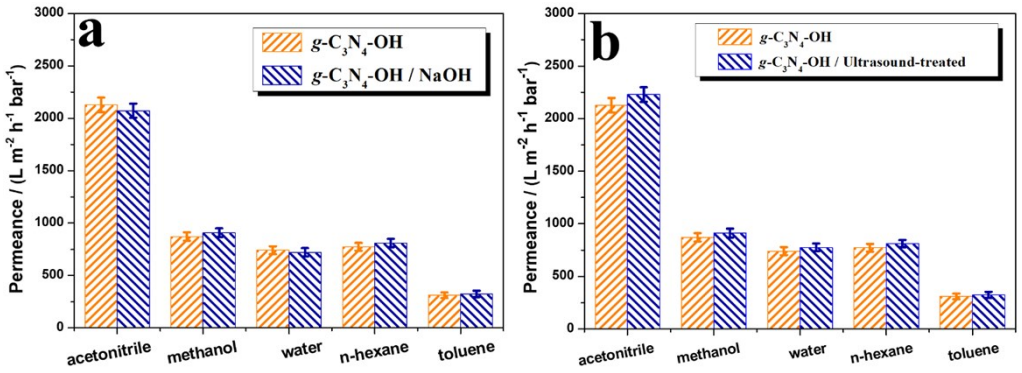

Fig. S31. Permeance change of acetonitrile, methanol, water, n-hexane, and toluene for *g*-C_3N_4-OH membrane after (a) soaking in HCl solution for 24 hours at pH = 4 and (b) ultrasonic 20 minutes in the test solution.

3. Supplementary Tables

Table S1 The chemical structures, molar weights and dimensional parameters of various dyes

Dyes	Mw (g/mol)	Chemical structure	Dimension (nm)	Electrical property
Methyl orange (MO)	327.3	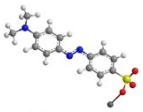	1.0	-
Methylene blue (MB)	373.9	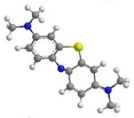	1.2	+
Crystal Violet (CV)	408.0	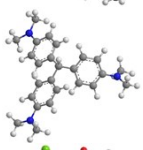	1.5	+
Reactive red (RR)	788.1	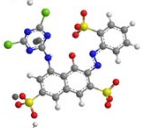	1.5	-
Brilliant Blue (BB)	792.9	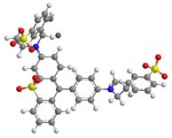	1.6	-
Acid yellow 14 (AY14)	449.2	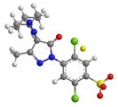	1.8	-

Table S2 Comparison of the separation performance for various membranes reported in literature.

Membrane	Thickness (nm)	Solute	Size (nm)	Rejection (%)	Permeance (L m^{-2} h^{-1} bar^{-1})			Reference
					acetone	methanol	water	
S-rGO-18	18	EB	3.1	100	-	77.2	90.2	4
HPEI/S-rGO-18	18	EB	3.1	100	-	72.5	-	4
rGO-TMPyP0.6-44	36.2	EB	3.1	100	27	5.1	9	2
uGNMs (GO)	53	MB	1.5	99.8	3.3	-	3.26	5
GO-RF8	500	MB	1.5	72	-	-	716	6
G-CNTm(2:1)/SA	40	MO	1.2	96	-	-	11	7
MoS_2 membrane	1700	EB	3.1	90	-	-	245	8
MoS2 membrane	2000	EB	3.1	90	-	-	160	8
MoS2 membrane	500	MB	1.5	90	-	-	45	9
PNIPAM-PBA/CCG	20	rhB	1.8	60	-	-	290	10
RGO-MWCNT(50)	570	MB	1.5	95	-	-	28	11
GOMs (GO)	1000	LR300	2.2	100	105	-	-	12
COF-LZU1	400	MB	1.5	99	-	-	760	13
COF-LZU1	400	MB	1.5	99	-	-	500	13
COF-LZU1	400	AF	1.7	91.4	-	-	570	13
COF-LZU1	400	rhB	1.8	99	-	-	380	13
g-C_3N_4 membrane	190	rhB	1.8	90	-	-	11.9	14
CDs-GO/MCE	2500	MB	1.5	94.1	-	-	439	15
SWCNT-intercalted GO	160	rhB	1.8	99	-	-	175	16
SWCNT-intercalted GO	40	rhB	1.8	97.4	-	-	270	16
Ag@MXene	470	rhB	1.8	79.9	-	-	387	17
GO-PVDF	50000	rhB	1.8	67.8	-	-	61.9	18
Shear-aligned GO	150	MB	1.5	99.5	-	-	71	19
NSC-GO	~2030	EB	3.1	83	-	-	573	20
HLGO	8	MB	1.5	95.5	12	9.8	48	1
GO	70	MB	1.5	96	-	0.6	2.8	1

Dyes abbreviation: evans blue (EB), methyl blue (MB), methyl orange (MO), rhodamine B (rhB), Lumogen Red 300 (LR300), acid fuchsin (AF).

4. Supplementary References

1 Q. Yang, Y. Su, C. Chi, C. T. Cherian, K. Huang, V. G. Kravets, F. C. Wang, J. C. Zhang, A. Pratt, A. N. Grigorenko, F. Guinea, A. K. Geim and R. R. Nair, *Nat. Mater.*, 2017, **16**, 1198−1202.

2 T. Gao, L. Huang, C. Li, G. Xu and G. Shi, *Carbon*, 2017, **124**, 263−270.

3 C. Chen, J. Wang, D. Liu, C. Yang, Y. Liu, R. S. Ruoff and W. Lei, *Nat. Commun.*, 2018, **9**, 1902.

4 L. Huang, J. Chen, T. Gao, M. Zhang, Y. Li, L. Dai, L. Qu and G. Shi, *Adv. Mater.*, 2016, **28**, 8669−8674.

5 Y. Han, Z. Xu and C. Gao, *Adv. Fun. Mater.*, 2013, **23**, 3693−3700.

6 C. S. Lee, M.-k. Choi, Y. Y. Hwang, H. Kim, M. K. Kim and Y. J. Lee, *Adv. Mater.*, 2018, **30**, 1705944.

7 Y. Han, Y Jiang and C. Gao, *ACS Appl. Mater. Interfaces*, 2015, **7**, 8147−8155.

8 L. Sun, H. Huang and X. Peng, *Chem. Commun.*, 2013, **49**, 10718−10720.

9 Z. Wang, Q. Tu, S. Zheng, J. J. Urban, S. Li and B. Mi, *Nano* Lett., 2017, **17**, 7289−7298.

10 Y. Wang, S. Chen, L. Qiu, K. Wang, H. Wang, G. P. Simon and D. Li, *Adv. Funct. Mater.*, 2015, **25**, 126–133.

11 K. Goh, W. Jiang, H. E. Karahan, S. Zhai, L. Wei, D. Yu, A. G. Fane, R. Wang and Y. Chen, *Adv. Funct. Mater.*, 2015, **25**, 7348–7359.

12 L. Huang, Y. Li, Q. Zhou, W. Yuan and G. Shi, *Adv. Mater.*, 2015, **27**, 3797–3802.

13 H. Fan, J. Gu, Hong. Meng, A. Knebel and J. Caro, *Angew. Chem., Int. Ed.*, *2018*, **57**, 4083–4087.

14 Y. Wang, L. Li, Y. Wei, J. Xue, H. Chen, L. Ding, J. Caro and H. Wang, *Angew. Chem., Int. Ed.* 2017, **56**, 8974 –8980.

15 W. Wang, E. Eftekhari, G. Zhu, X. Zhang, Z. Yan and Q. Li, *Chem. Commun.*, 2014, **50**, 13089–13092.

16 S. Gao, H. Qin, P. Liu and J. Jin, *J. Mater. Chem. A*, 2015, **3**, 6649–6654.

17 R. P. Pandey, K. Rasool, V. E. Madhavan, B. Aïssa, Y. Gogotsi and K. A. Mahmoud, *J. Mater. Chem. A*, 2018, **6**, 3522–3533.

18 Z. Zhu, L. Wang, Y. Xu, Q. Li, J. Jiang and X. Wang, *Adv. Colloid Interf. Sci.*, 2017, **504**, 429–439.

19 A. Akbari, Phillip. Sheath, S. T. Martin, D. B. Shinde, M. Shaibani, P. C. Banerjee, R. Tkacz, D. Bhattacharyya and M. Majumder, *Nat. Commun.*, 2016, **7**, 10891.

20 H. Huang, Z. Song, N. Wei, Li. Shi, Y. Mao, Y. Ying, L. Sun, Z. Xu and X. Peng, *Nat. Commun.*, 2013, **4**, 2979.